A Sequence-Anchored Linkage Map of the Plant–Parasitic Nematode *Meloidogyne hapla* Reveals Exceptionally High Genome-Wide Recombination

Varghese P. Thomas,*,[1] Sylwia L. Fudali,* Jennifer E. Schaff,[†] Qingli Liu,*,[2] Elizabeth H. Scholl,[‡] Charles H. Opperman,[‡] David McK. Bird,[‡,§] and Valerie M. Williamson*,[3]

*Department of Nematology, University of California, Davis, California 95616, and [†]Genome Sciences Laboratory, [‡]Department of Plant Pathology, and [§]Bioinformatics Research Center, North Carolina State University, Raleigh, North Carolina 27695

ABSTRACT Root-knot nematodes (*Meloidogyne* spp.) cause major yield losses to many of the world's crops, but efforts to understand how these pests recognize and interact with their hosts have been hampered by a lack of genetic resources. Starting with progeny of a cross between inbred strains (VW8 and VW9) of *Meloidogyne hapla* that differed in host range and behavioral traits, we exploited the novel, facultative meiotic parthenogenic reproductive mode of this species to produce a genetic linkage map. Molecular markers were derived from SNPs identified between the sequenced and annotated VW9 genome and *de novo* sequence of VW8. Genotypes were assessed in 183 F2 lines. The colinearity of the genetic and physical maps supported the veracity of both. Analysis of local crossover intervals revealed that the average recombination rate is exceptionally high compared with that in other metazoans. In addition, F2 lines are largely homozygous for markers flanking crossover points, and thus resemble recombinant inbred lines. We suggest that the unusually high recombination rate may be an adaptation to generate within-population genetic diversity in this organism. This work presents the most comprehensive linkage map of a parasitic nematode to date and, together with genomic and transcript sequence resources, empowers *M. hapla* as a tractable model. Alongside the molecular map, these progeny lines can be used for analyses of genome organization and the inheritance of phenotypic traits that have key functions in modulating parasitism, behavior, and survival and for the eventual identification of the responsible genes.

KEYWORDS
root-knot nematode
SNP
integrated map

Despite continued intrusion of agriculture into natural ecosystems, world food production is increasingly falling short of demand. Concomitantly, traditional farmlands are becoming less arable due to salinity, nitrogen pollution, erosion, and many other factors. In a recent analysis, Foley *et al.* (2011) proposed four broad approaches to mitigate the impending global food crisis, including, not surprisingly, increasing crop yield. One direct route to this goal is to control yield-reducing pests. Because of their enormous impact, plant parasitic nematodes are a significant target, although often neglected. Collectively, nematodes are responsible for more than $100 billion annual crop loss worldwide, and root-knot nematodes (RKN; genus *Meloidogyne*) are generally considered the most damaging (Chitwood 2003; Roberts 1995; Sasser and Freckman 1987; Sasser 1980; Trudgill and Blok 2001).

RKN are obligate endoparasites with a specialized life cycle that is characterized by developmental reprogramming of host tissue to form multinucleate giant cells (GC) from which the parasite feeds (Williamson and Gleason 2003). Attempts to identify nematode genes

doi: 10.1534/g3.112.002261
Manuscript received February 23, 2012; accepted for publication May 10, 2012

Supporting information is available online at http://www.g3journal.org/lookup/suppl/doi:10.1534/g3.112.002261/-/DC1
[1]Present address: AgraQuest Inc., Davis, CA 95618.
[2]Present address: Syngenta Biotechnology Inc., Durham, NC 27709
[3]Corresponding author: Dept. of Plant Pathology, One Shields Ave., University of California, Davis, CA 95616. E-mail: vmwilliamson@ucdavis.edu

responsible for infection and feeding site development and maintenance have focused largely on analysis of secreted molecules and the genes that encode them (Bellafiore *et al.* 2008; Davis *et al.* 2008). RKN produces an extensive secreted proteome that includes enzymes able to degrade plant cell walls, such as β-1, 4-endoglucanases (cellulase), pectate lyase, and exo-polygalacturonase. These enzymes likely facilitate nematode migration within the roots and additionally may play a role in feeding site formation and maintenance (Davis *et al.* 2008; Popeijus *et al.* 2000). Other secreted proteins, including chorismate mutase, may modulate metabolites, leading to immune suppression and modified root cell morphology (Lambert *et al.* 1999). RKN mimics of the recently discovered class of plant peptide hormone called RAR (root architecture regulators) also appear to play a role in directly regulating feeding site formation (D. M. Bird, unpublished data). However, without functional analyses, the role of these genes in the host-parasite interaction remains untested. To redress this shortcoming, we have developed forward genetics for *Meloidogyne hapla* permitting the identification, mapping, and isolation of genes based on phenotype alone.

To date, genetic resources for parasitic nematodes have been limited (Sommer and Streit 2011). Because they have a free-living stage that can be maintained *in vitro*, certain Strongylid species have been proposed as genetic models, but various limitations have hindered the development of these systems (Viney and Lok 2007). More progress has been made with plant-parasitic nematodes, particularly cyst nematodes species, where screening progeny of controlled crosses with molecular markers has allowed production of genetic maps (Atibalentja *et al.* 2005; Dong and Opperman 1997; Rouppe van der Voort *et al.* 1999). However, these maps are low resolution, and the genetic systems they underpin are limited in utility due to biological barriers, such as the obligate outcrossing reproductive mode and inbreeding depression of the nematode species used. In contrast, most populations of *M. hapla* are diploid and reproduce by facultative meiotic parthenogenesis; sexual crosses can occur, but parthenogenetic progeny are also produced. The ability to experimentally toggle between these modes empowers *M. hapla* as a genetic model. Beyond that, *M. hapla* is a major parasite of tomato, potato, carrot, lettuce, alfalfa, onion, and a multitude of other crops (Mitkowski *et al.* 2002), and it causes significant damage in temperate regions worldwide. Wild isolates of *M. hapla* display extensive phenotypic differences germane to the host-parasite interaction, providing the sources of variability crucial to genetic analysis. Examples include differences in host range and pathogenicity (Liu and Williamson 2006) and the ability to overcome resistance in diverse species, including alfalfa (*Medicago sativa*) (Griffin and McKenry 1989), *Solanum* spp. (Janssen *et al.* 1997; Van der Beek *et al.* 1998;), and common bean (*Phaseolus vulgaris*) (Chen and Roberts 2003). Comparison of *M. hapla* strains using AFLP (Vos *et al.* 1995) showed that approximately 4% of fragments were polymorphic between strains (Liu and Williamson 2006); thus, observed phenotypic diversity reflects an underlying molecular variability and provides the basis for our comprehensive genetic assessment. Genetic studies have shown segregation patterns in *M. hapla* consistent with monogenic inheritance for a trait conferring ability to reproduce on common bean carrying a nematode-resistant gene (Chen and Roberts 2003) and for a trait modulating clumping behavior (*Clm*) (Wang *et al.* 2010).

For *M. hapla*, as for many RKN species, sex is environmentally influenced (Triantaphyllou 1973). At hatch, RKN are determined to become oocyte-producing adults with a female soma. Under favorable conditions for the nematode, males are rare or absent and reproduction is asexual. Male development is initiated after infection and is promoted by unfavorable conditions, such as crowding and poor nutrition. Motile adult males exit the root and mate with sedentary females. Sperm are stored in the spermatheca and are competent to fertilize oocytes, stimulating meiotic maturation and resulting in production of hybrid, diploid progeny (Figure 1A). In the gonads of unfertilized females, meiosis occurs, but meiotic progression is prolonged (Figure 1B). Restoration of diploidy occurs by rejoining of sister chromosomes of a single meiosis to produce a cell that is functionally equivalent to a zygote (Liu *et al.* 2007; Triantaphyllou 1966).

The development of two highly inbred *M. hapla* strains, *viz.*, VW8 and VW9, which differ in pathogenicity phenotypes and DNA markers, has been described elsewhere (Liu and Williamson 2006); a high-quality draft sequence of the VW9 genome is publicly available (www.hapla.org) (Opperman *et al.* 2008). As a starting point for genetic analysis, we performed a cross between VW8 and VW9 (Liu *et al.*, 2007). A set of 183 F2 lines was established, each descended from the brood of a single F2 female (Figure 1C). These lines were maintained as separate cultures on tomato plants. Analysis of AFLP marker segregation in these lines resulted in the production of a genetic map distributed over 15 linkage groups (LG) (Opperman *et al.* 2008). Here we report two strategies to anchor the genetic map to the sequence scaffolds, *viz.*, sequencing mapped AFLP fragments and mapping single nucleotide polymorphisms (SNP) that differ between parental strains. This integrated map reveals that *M. hapla* has an unusually high recombination rate. Additionally, the integrated genetic/genomic map and F2 lines provide powerful tools for identifying and cloning genes conferring functional differences in parasitism and other traits of interest.

MATERIALS AND METHODS

Nematode cultures

The inbred strains of *M. hapla* and 183 F2 lines from the cross VW8xVW9 (Liu *et al.* 2007) were maintained on tomato (*Solanum lycopersicum*) cultivar VFNT in a greenhouse at the University of California, Davis, CA. Nematode eggs were isolated from roots, cleaned and DNA extracted as previously described (Liu and Williamson 2006).

Isolation and sequencing of AFLP fragments

AFLP fragments were excised from dried polyacrylamide gels produced in previous F2 analysis (Opperman *et al.* 2008) using a protocol described in Liu and Williamson (2006). For weak or small fragments, the DNA was further concentrated using a QIAquick Gel Extraction Kit (Qiagen). In the final step, the DNA was eluted in 20 μl of TE, pH 8.0, or water and stored at −20°. The isolated DNA fragments were reamplified by PCR as previously described (Liu and Williamson 2006). PCR products were separated on a 1.2% agarose gel and purified using QIAquick Gel Extraction kit, and then cloned into the pGEM-T easy vector (Promega Corp, Madison, WI). Clones with the expected insert size were sequenced at the UC Davis, College of Biological Sciences Sequencing Facility. AFLP marker sequences were compared with the VW9 genome sequence using BlastN with low complexity filtering turned off and a significance threshold of $1.0e^{-10}$. Only sequenced AFLP fragments that were unique to the genome sequence and matched genomic sequence along their entire length were assigned to contigs.

SNP marker development and genotyping

The Illumina GoldenGate Assay (Illumina Inc., San Diego, CA), BeadXpress platform, was used for SNP genotyping of DNA (Fan *et al.*, 2003). To identify SNP polymorphisms, a 2.3× coverage (125 Mb)

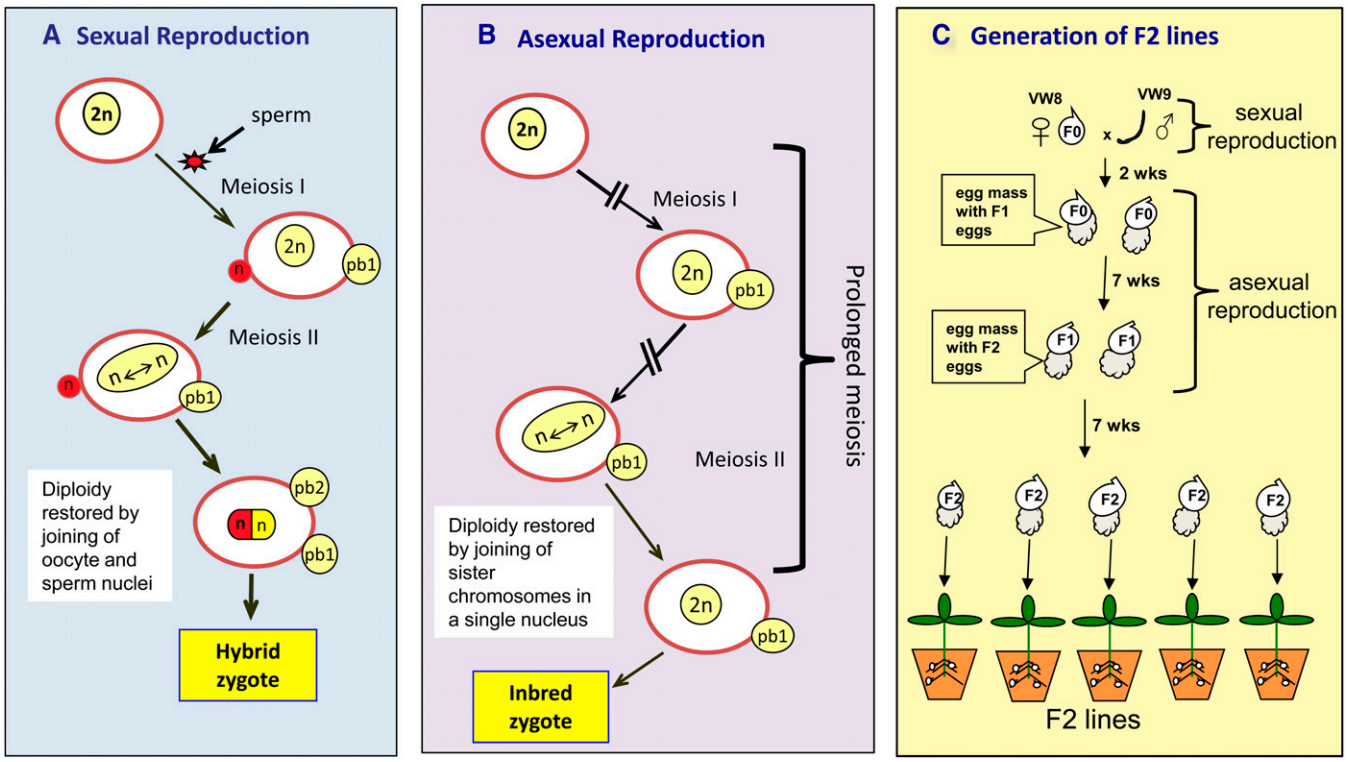

Figure 1 Strategy used to produce *Meloidogyne hapla* F2 lines. Panels A and B compare meiotic progress of oocytes (white ovals) in the presence or absence of sperm, starting with prophase I. Development prior to prophase I, where recombination is thought to occur, appears the same for sexual and asexual reproduction (Liu *et al.* 2007). In sexual reproduction (A), sperm (red) are present in the spermatheca and fertilize the female gamete, promoting completion of meiosis and resulting in a hybrid zygote. In asexual reproduction (B), meiotic maturation is prolonged. Diploidy is reestablished by the joining of sister chromosomes of meiosis II, resulting in an inbred zygote. Yellow circles represent maternal genome (2n) and polar bodies 1 and 2 (pb1 and pb2). Paternally derived genome is diagrammed in red. To generate F2 lines (panel C), females of VW8 were mated with males of VW9. Eggs from mated females (F0) were hatched, and juveniles were allowed to infect roots and develop into F1 (hybrid) females. These F1 females were allowed to reproduce asexually to produce an egg mass containing F2 eggs. Eggs are produced by the female beginning at about 4 weeks post infection; the egg mass containing the collective progeny of a female is collected at 7 weeks post infection. Each F2 line was initiated with a single egg mass, which comprises the progeny of a single F2 female. See Liu *et al.* (2007) for details.

sequence was produced using the 454 GS FLX platform from DNA extracted from a pool of 10 randomly selected F2 lines from the VW8 × VW9 cross. Pooled DNA was used rather than parental DNA to more directly reflect the alleles present in the F2 lines. SNP candidates that had at least two iterations of the deduced VW8 sequence and that were flanked by 60 nt of nonpolymorphic sequence were selected. Candidate SNPs were selected to include those on large sequence contigs or contigs containing genes of interest. In several cases, more than one SNP was chosen per contig. Candidate SNPs were assigned a "designability" rank score by Illumina, and only those with a score of >0.6 were selected to be included in the oligo pool assay. DNA from the same set of F2 lines used in genetic map construction (Liu *et al.* 2007; Opperman *et al.* 2008) was used for SNP genotyping. Samples were aliquoted into two 96-well plates with one F2 line in duplicate in each plate to verify genotype reproducibility. Assays were carried out at the UC Davis Genome Center, DNA Technologies Core Facility. Scoring of SNP genotypes was performed using the Illumina BeadStudio 3.2 genotyping software. Genotype calling for each SNP was rechecked manually and rescored if necessary to optimize clustering of progeny categories. Candidate SNPs that were monomorphic, failed to amplify, or did not form well-resolved genotypic groupings were excluded. SNP markers are annotated with the letter "C" followed by the contig number and the position of the polymorphism on the contig (www.hapla.org).

Segregation analysis and linkage map generation

Linkage maps were produced using JoinMap v4.0 (Stam 1993; Van Ooijen 2006). As none of the available data type options were a match for our segregating population type, we used the data type DH1 (double haploid) as a best approximation. Individuals were genotyped as "A" when they were homozygous for the maternal parent (VW8) allele and "B" when homozygous for the parental male (VW9) allele. Because DH1 does not accommodate heterozygotes, we assigned "U" (missing data) for markers that were scored as heterozygotes. The markers were assigned to LGs based on the logarithm of odds (LOD) ratio for each marker pair. A minimum threshold LOD value of 3.0 was initially used to generate LGs and the final groupings were at LOD ≥ 7.0. Default mapping parameters were used to order markers in LGs, and the Kosambi mapping function was used to convert the recombination frequencies into map distances in centimorgans (cM). MapChart v2.2 software (Voorrips 2002) was used for the graphical visualization of the linkage groups. Fit to 1:1 segregation was assessed using a chi-square goodness-of-fit (χ^2) test, and the *P* value was recorded.

RESULTS

Identification of sequence-anchored markers

A total of 80 unique DNA fragments spanning AFLP markers were isolated and sequenced. Of these, 12 were removed because they did not align to genomic sequences along their entire length or consisted of low complexity sequences. The remaining 68 sequenced AFLP markers were assigned to contigs, but because 15 of these were codominant (allelic) markers, this corresponded to 53 loci (supporting information, Table S1).

As a second strategy to obtain anchored markers, we identified SNPs between the parental strains and genotyped SNP alleles in the F2 lines by comparison of the annotated VW9 genome sequence to a 2.3× sequence of 10 pooled F2 lines. This strategy identified more than 21,000 putative SNPs between the two parental strains. A total of 192 candidate SNPs were processed using the Illumina GoldenGate platform and 132 markers were successfully genotyped (Table S2). Consistent with our previous findings using a limited number of codominant AFLP markers (Liu *et al.* 2007), genotyping of F2 lines revealed that SNP markers displayed predominantly a two-grouping pattern, indicating that heterozygotes were vastly underrepresented and most loci were homozygous for one or the other parental type. The fraction of heterozygotes ranged from 0 to 10.9% (mean = 3.9%), depending on the SNP marker (Table S2).

Generating a genetic linkage map

A genetic linkage map was generated using (a) 132 SNP markers that were successfully genotyped in the 183 F2 lines, (b) AFLPs anchored to contigs, and (c) additional AFLP markers, which were individually selected to increase the marker density between SNPs and to allow comparison between the previous AFLP-based map and the current map (Figure 2). The phenotypic trait for clumping (*Clm*) that segregated in the F2 lines was also included (Wang *et al.* 2010). The resultant map displays 16 LGs with 8 or more markers, corresponding to the haploid complement of 16 chromosomes predicted by karyotyping (Liu and Williamson 2006). Three additional groupings, each with only 2–3 markers were identified and presumably represent orphaned fragments of the larger linkage groups. Linkage groups were numbered to correspond to the previously published AFLP-based map (Opperman *et al.* 2008). Linkage groupings were maintained between the two map versions with only a few exceptions. Although the marker density varies within and between linkage groups, there are only two gaps of >20 cM, both on LG11. Differences in marker density may be partially explained by the differences in chromosome size. Measurements of pachytene chromosomes in a *M. hapla* female indicated that chromosomes vary over 3-fold in length (Goldstein and Triantaphyllou 1978).

Anchoring the physical and genetic linkage maps

The *M. hapla* genome assembly is represented by 1523 scaffolds (www.hapla.org); scaffolds are sets of ordered contigs connected by contiguous sequence, although not all of that sequence may be known (Opperman *et al.* 2008). By placing 182 markers on the map (Table 1), we anchored 138 sequenced contigs (representing 117 scaffolds). Among the 132 mapped SNP markers, only 3 did not map to the same genetic position as other markers on the same scaffold, reflective of the integrity of the genetic and physical maps (Table S2). Although genome-wide correlative data are limited due to the relatively few integrated markers and gaps in the genome assembly, comparisons so far indicate that the genetic and physical maps are colinear. For example, all of the sequenced markers on LG15 are on contigs present in the same order as on the 655,672 bp Scaffold 0, the longest sequence scaffold in the genome, and all anchored markers identified as being on Scaffold 0 map to LG15 (Figure 3). Similarly, the 5 anchored contigs on Scaffold 3 map to LG8 in the same order (Figure 3).

Estimates of recombination rate

The genotype analysis included 22 pairs of SNPs at physically separated positions on long contigs that map to 12 different linkage groups. To estimate the recombination rate between each pair of SNPs, we calculated the percentage of recombinant chromosome intervals from the genotypes of individuals in the F2 population (Table 2). Using the percentage recombination as an estimate of the genetic distance in cM and the known physical distance between the SNPs, we calculated local recombination rates for these intervals ranging from 34.6 to 372 cM/Mb (Table 2).

Positioning genes on linkage groups using the integrated map

As a demonstration of the utility of the integrated genetic map/genome sequence, we assessed the organization of two gene families hypothesized to have been acquired by horizontal gene transfer (HGT; Scholl *et al.* 2003): the gene families that encode the pectate lyases (PL) and β-endoglucanase. The *M. hapla* genome encodes 22 PL genes, some of which are grouped on contigs in patterns consistent with tandem duplication (Opperman *et al.* 2008). Phylogenetic reconstruction of PLs in *M. hapla* as well as other plant parasitic nematodes, bacteria, fungi, and oomycetes suggests that progenitors were acquired by nematodes from bacteria through at least two independent HGT events (Opperman *et al.* 2008; Danchin *et al.* 2010). By comparing the annotated position on a sequence scaffold of each PL gene to the anchored markers, we were able to localize 16 PL genes to linkage groups (Figure 4). Eight of the genes mapped to LG2 and five mapped to LG13, with copies belonging to the same clade found predominantly on the same linkage group (Figure 4). The genetic clustering of clades is consistent with the hypothesis that expansion of the gene family occurred by duplications preferentially on the same linkage group. Using the same strategy, we positioned 6 cellulase genes on the genetic map (Figure 4). At least 4 of these map to LG6, again suggesting localized duplication events were involved in the expansion of these gene families. We note that these two gene families, although both are likely involved in parasitism, do not colocalize in the nematode genome. As the map becomes more marker-dense, additional information on genome-wide organization of parasitism genes as well as information on their patterns of expansion in the genome will become available.

Regions with distorted segregation

Segregation of some markers deviated from a 1:1 ratio in F2 lines in the previous AFLP-based map (Opperman *et al.* 2008), but the scope of that analysis was limited due to the paucity of codominant markers. In the current study, χ^2 analysis of genotype frequencies revealed that about a third of the loci deviate significantly from the 1:1 ratio ($P < 0.05$) (Figure 2). These loci are clustered on several linkage groups. Interestingly, loci on LG6 are biased toward the female parent (*M. hapla* strain VW8), whereas those on LG2, 5, 8, and 16 are biased toward the male parent (VW9).

DISCUSSION

Despite considerable effort spent in attempting to establish tractable genetic systems for parasitic nematodes, previous success has been

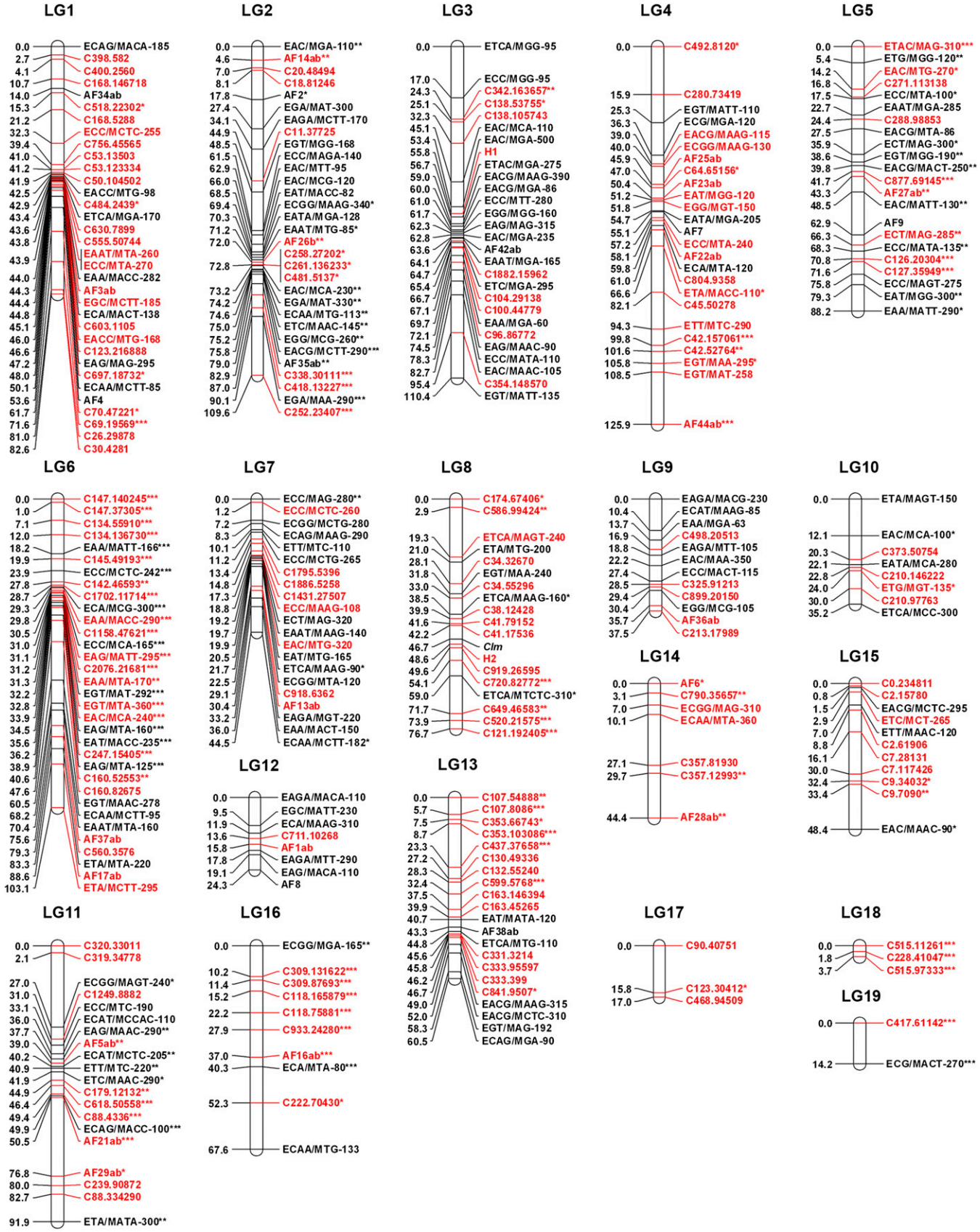

Figure 2 Genetic linkage map of *Meloidogyne hapla* based on SNP and AFLP markers. This map is based on segregation of markers in 183 F2 lines; LGs were generated using JoinMap 4.0. Markers anchored to genome sequence are shown in red and are listed in Table S1 and Table S2. Markers showing segregation ratios that deviate significantly from 1:1 are indicated with $^{*}P < 0.05$, $^{**}P < 0.01$, or $^{***}P < 0.001$.

Table 1 Summary of linkage group features

LG	# Sequenced AFLP Loci	# SNP Loci	# Contigs Anchored	Mb Spanned by Contigs	# Scaffolds Anchored	Mb Spanned by Scaffolds
1	6	19	22	1.83	18	2.93
2	2	9	10	0.84	7	1.48
3	1	8	8	0.83	6	0.99
4	13	7	13	0.93	10	2.00
5	4	5	6	0.63	5	0.86
6	8	13	14	0.97	15	2.25
7	4	4	7	0.30	7	0.57
8	2	12	11	1.02	9	1.65
9	1	4	4	0.38	4	0.58
10	1	3	2	0.31	2	0.37
11	3	8	9	0.91	8	1.17
12	1	1	2	0.04	2	0.19
13	0	14	10	1.05	8	1.55
14	4	3	5	0.19	4	0.29
15	1	7	4	0.52	1	0.66
16	1	6	5	0.65	5	0.82
17	0	3	3	0.51	3	0.83
18	0	3	2	0.19	2	0.32
19	0	1	1	0.07	1	0.15
Total	52	130	138	12.17	117	19.66

limited. The system described herein contains a nearly complete set of genetic tools for examination of parasite biology and host interaction, and it represents a major advance in the study of parasitic nematodes.

The availability of a robust genome sequence draft combined with an integrated genetic map establishes *M. hapla* as model system to study fundamental questions pertaining to parasitism. With the use of codominant SNP-based markers, we have produced a robust genetic map showing excellent congruence in marker order between the map and genome assembly. This map is a highly developed resource, and it has begun to yield information on the genome organization, such as we show here for the PL and cellulase gene families.

To explain the paucity of heterozygotes, we previously suggested, based on limited data with AFLP markers, that *M. hapla* has a novel mechanism of chromosome resolution in which recombination occurs on all four strands at similar locations (Liu *et al.* 2007). Examination of codominant SNP markers flanking crossovers on the same contig in individual F2 lines revealed that in the majority of cases these markers are homozygous (Table 2), supporting the widespread occurrence of four-strand crossovers. We also suggested previously that the crossovers occur at similar, but not identical, locations for the two pairs of sister chromosomes. Genotype data from SNP pairs in F2 lines supports this model, as heterozygous alleles are more prevalent adjacent to crossovers than in the genome on average (Table 2). However, four-strand crossovers such as we have proposed have the potential to be detrimental to chromosome cohesion and thus could lead to improper segregation in meiosis I. In addition, other explanations, also largely unprecedented, such as premeiotic recombination (*e.g.* before meiotic chromosome replication), could produce results similar to what we have found. Additional studies will be required to clarify the mechanisms responsible for the observed recombination patterns. On

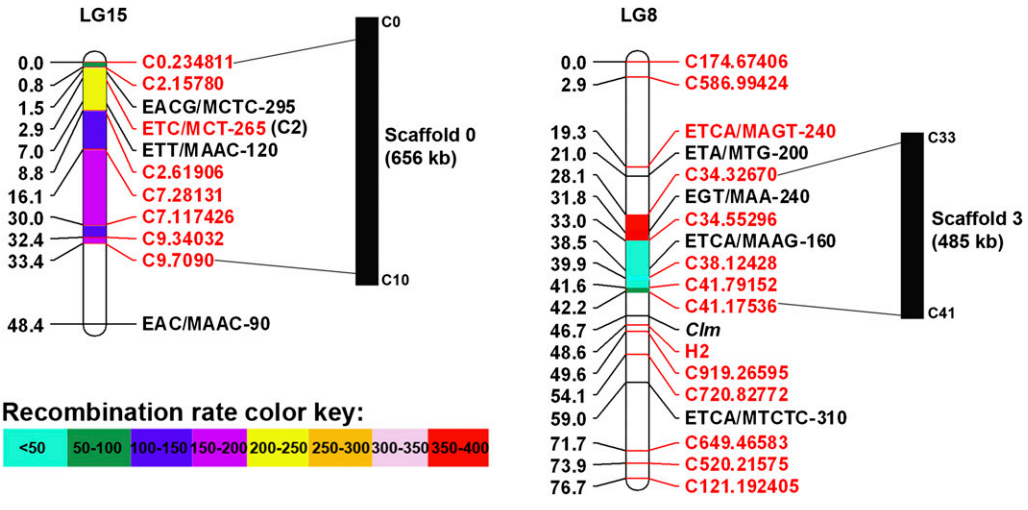

Figure 3 Colinearity of genetic and physical maps. The genetic map of LG15 is compared to Scaffold 0. At more than 650 kb, Scaffold 0 is the longest in the current assembly and contains contigs C0 to C10. Contigs are numbered in ascending order based on their relative physical position on the scaffold. Comparison of map of LG8 to Scaffold 3, which contains contigs C33 to C41. For both Scaffold 0 and Scaffold 3, the physical order of the contigs corresponds to their genetic order, supporting colinearity of the genetic and physical maps. Recombination rates between anchored markers are indicated on the LG according to the color key.

Table 2 Recombination rate between SNP marker pairs on individual contigs

LG	Marker 1	Marker 2	JoinMap Distance (cM)	Physical Distance (Kb)	Number of Lines of Each Genotype (Marker 1/Marker 2)										Calculated Genetic Distance (cM)[b]	Rec. Rate (cM/Mb)[c]
					AA/AA	BB/BB	AB/AB	AA/BB	BB/AA	AB/AA	AB/BB	AA/AB	BB/AB	U[a]		
1	C168.5288	C168.146718	10.5	141.4	62	78	5	14	6	3	5	5	5	0	15.8	111.7
1	C53.13503	C53.123334	0.2	109.8	79	89	0	1	1	5	1	2	5	0	4.6	41.9
3	C138.53755	C138.105743	7.2	51.9	66	88	0	6	7	3	3	1	9	0	11.4	264.0
4	C42.52764	C42.157061	1.8	104.3	63	110	1	3	1	0	2	3	0	0	3.6	34.6
6	C147.37305	C147.140245	1.0	102.9	124	47	0	2	0	0	6	4	0	0	3.8	36.9
6	C134.55910	C134.136730	4.9	80.8	118	44	6	4	3	3	0	2	3	0	6.0	74.2
6	C160.52553	C160.82675	7.0	30.1	90	58	3	11	1	3	2	6	5	4	11.2	372.1
8	C34.32670	C34.55296	4.9	22.6	79	83	0	9	0	1	6	5	0	0	8.2	362.9
8	C41.17536	C41.79152	0.6	61.6	78	90	1	3	0	7	2	0	2	0	4.6	74.7
10	C210.97763	C210.146222	7.2	48.4	72	87	9	10	3	0	0	0	2	0	8.2	169.4
11	C88.4336	C88.334290	33.3	329.9	39	74	1	12	43	3	3	1	7	0	33.9	103.0
13	C107.8086	C107.54888	5.7	46.8	58	100	1	7	2	7	1	0	7	0	9.0	192.3
13	C353.66743	C353.103086	1.2	36.3	67	105	0	4	0	0	4	2	0	1	3.8	104.7
13	C333.399	C333.95597	0.4	95.1	68	90	1	0	1	8	6	4	5	0	6.8	71.5
13	C163.45265	C163.146394	2.4	101.1	84	75	7	4	0	2	3	1	7	0	5.7	56.4
14	C357.12993	C357.81930	2.6	68.9	71	99	0	0	5	6	0	0	2	0	4.9	71.1
15	C9.7090	C9.34032	1.0	26.9	67	97	2	2	1	5	1	0	7	1	5.2	193.3
15	C7.28131	C7.117426	13.9	89.2	60	75	7	7	11	3	7	5	8	0	16.1	180.5
15	C2.15780	C2.61906	8.0	46.1	74	81	2	9	1	1	8	4	3	0	9.8	212.6
16	C309.87693	C309.131622	1.2	43.9	62	111	1	0	3	0	0	1	4	1	3.0	68.3
16	C118.75881	C118.165879	7.0	89.9	50	107	4	6	7	1	5	3	0	0	9.6	106.8
18	C515.11261	C515.97333	3.7	86.1	50	111	2	3	2	6	1	3	4	1	6.5	75.5

[a] Number of individuals for which marker genotypes were not available.
[b] Genetic distance estimates derived by calculating the percent recombinants in the F2 lines.
[c] The recombination rate shown uses the calculated values for genetic distance.

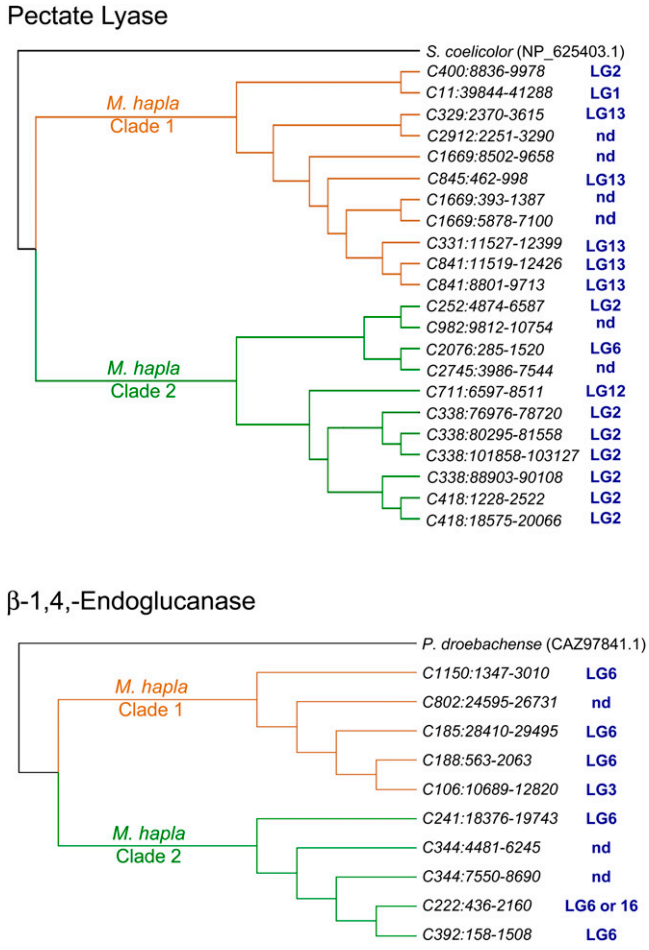

Figure 4 Genomic organization of pectate lyase and endoglucanase genes. Phylogenetic trees were created using protein distance and neighbor joining on 10,000 bootstrapped replicates. The consensus trees are displayed with gene copies identified by contig and position on contig. Linkage group assignments (blue font) were deduced from colocalization of coding region with mapped SNPs on the same scaffold. Genes that we were unable to assign to a linkage group are indicated by "nd." The genetic location of Scaffold 36, which includes Contig 222, is ambiguous: Contig 224 (based on AFLP markers AF37a/b) places Scaffold 36 on LG6, but SNP C222.70430 places it on LG16.

a practical level, because of the homozygosity of most loci, F2 lines resemble recombinant inbred lines and should be genetically uniform, facilitating mapping and cloning of genes responsible for the associated traits.

Although the marker order in the genetic map and sequence scaffold are highly congruous, the current map generated by JoinMap underestimates genetic distances. Comparison of the manually calculated local genetic distances for the 22 SNP pairs shown with the genetic distances calculated by JoinMap illustrates this (Table 2). In all cases, the distance between the SNP markers calculated by JoinMap is lower: in some cases only slightly lower, but in others, the JoinMap value is 20-fold lower. This discrepancy indicates that the algorithms used by JoinMap make assumptions regarding recombination and its resolution that do not accurately reflect the situation in our novel system. For example, none of the options incorporates the unprecedented positive crossover interference that we propose. The JoinMap program bases gene order on regression mapping (Stam 1993), and mean recombination frequencies are generated for all pairs of loci on a linkage group. We used the Kosambi mapping function option to convert the recombination frequencies into centimorgans. We also explored several different mapping parameter and population type options of JoinMap; all produced very similar gene order and none produced genetic distances that reflected the calculated local recombination distances. As more data become available from additional crosses and marker analysis, we should be able to better optimize mapping parameters to more accurately reflect genetic distances for our system.

Using the average of the calculated recombination rates for 22 SNP pairs distributed over 12 linkage groups, we estimate the genome-wide recombination rate to be 135 cM/Mb. This estimate assumes that these 22 local rates represent a more or less random sampling of the genome. In *Caenorhabditis elegans*, recombination rates show a pattern of high rates in chromosome arms and low, relatively uniform rates in the central region of the chromosome (Barnes *et al.*., 1995; Rockman and Kruglyak 2009). Although the local rates that we see for *M. hapla* differ by as much as 10-fold, we see no obvious correlation of rate with linkage group. However, due to gaps in the physical assembly, we are not yet able carry out an analysis of chromosome-wide distribution of recombination rates. Examination of recombination rates between anchored markers in the two sequence scaffolds for which we have the most information suggests that the chromosome-wide pattern of recombination will be complex, with intermixing of high and low rates (Figure 3). Analysis of a denser SNP map and additional lines will be necessary to obtain an accurate picture of the distribution of crossover frequencies along the chromosomes. If the estimate of 135 cM/Mb in fact approximates the genome-wide recombination rate, *M. hapla* has the highest recombination rate for any metazoan reported to date. For comparison, the mean genome-wide recombination rate in *C. elegans* is 2.7 cM/Mb, for *Drosophila*, it is 1.6 cM/Mb, and for the honeybee, *Apis mellifera*, which has the highest previously reported value for a metazoan, the genome-wide recombination rate is only 22 cM/Mb, although recombination rate in honeybee also ranges as high as 143 cM/Mb in certain areas of the genome (Beye *et al.* 2006; Solignac *et al.* 2007).

Similar recombination rate values to *M. hapla* have been reported for parasitic protozoans, including *Plasmodium falciparum* (Su *et al.* 1999), *Trypanosoma brucei* (Macleod *et al.* 2005), and *Theileria parva* (Katzer *et al.* 2011), suggesting the intriguing possibility that this is an adaptation to the obligate parasite lifestyle. It has been suggested that organisms with extended asexual periods of reproduction could benefit from increased recombination (Wilfert *et al.* 2007). Adaptive evolution of recombination frequency provides several advantages to the obligate parasite, including increasing diversity in the short term to benefit a population with restricted migration and population mixing. Increased local recombination can also reduce linkage drag, which in turn may enhance adaptation and multilocus selection (Hill and Robertson 1966). Whether the novel mode and mechanism of chromosome recombination that we see in this *M. hapla* cross extends to other RKN species remains to be determined. However, cytological studies show that meiotic parthenogenesis occurs in several other *Meloidogyne* species (Van der Beek *et al.* 1998; Triantaphyllou and Hirschmann 1980). Although so far our understanding about how and when recombination occurs and how crossovers are resolved in these species is limited, on a practical level, the high recombination frequency will facilitate localizing and cloning genes corresponding to phenotypes of interest that segregate in F2 lines.

The small genome size together with the relatively large chromosome complement may contribute to the high recombination rate of *M. hapla*. The average chromosome size is predicted to be ~3 Mb,

and for most organisms, at least one crossover per chromosome pair is thought to be required and 1.6 crossovers per chromosome may be more typical (Baker *et al.* 1976). Whereas for *C. elegans*, one and only one crossover per chromosome pair in meiosis is thought to occur (Hillers and Villeneuve 2003), this does not appear to be the case for *M. hapla*, where the length of several linkage groups is ~100 cM, consistent with approximately one crossover per chromosome (two per pair). If the current genetic map is compressed, as we suggest above, the number of crossovers per linkage group in *M. hapla* may be even higher than two. Although the number of major linkage groups and chromosomes is the same and high LOD scores support these groupings, we cannot be certain that in all cases the genetic linkage groups correspond to physical chromosomes. A few gaps of >20 cM and three groupings with 2–3 markers each remain that are not yet associated with the putative chromosomes. Additional markers and genetic crosses should eventually resolve these ambiguities. Two additional tools to assess correspondence between linkage groups and chromosomes are fluorescent *in situ* hybridization and pulsed field gel electrophoresis to separate chromosomes, but neither of these has been successful for root-knot nematodes so far.

Although segregation of alleles was approximately 1:1 for the majority of loci, for about a third of the loci, allele frequency was skewed toward one of the parental alleles. Segregation distortion has been observed in a broad range of organisms and has been attributed to a range of causes, including meiotic selection driven by the presence of particular alleles during meiosis (Taylor and Ingvarsson 2003). In *C. briggsae*, analysis of recombinant inbred lines derived from crosses between divergent strain pairs found that cytonuclear epistasis and differences in development rate mediated by particular alleles or allele combinations are factors (Ross *et al.* 2011). In the steps required to produce our F2 lines (Figure 1C), there are several additional points at which segregation distortion could be manifested. To produce an F2 line, the egg from the F1 female must hatch, the emerged juvenile needs to migrate through the soil, infect a host root, establish a feeding site, and successfully produce progeny. Allele differences that contribute to relative success at any of these points could lead to segregation distortion. For example, because we use tomato as a host, juveniles that are more attracted to tomato roots may be favored. With additional analysis, the distorted segregation may direct us to genes involved in nematode fitness, survival, or parasitism.

Models have proved to be invaluable tools to elucidate biological understanding of less-tractable organisms (Bird 2005), and *M. hapla* has features that make it a powerful model. However, because *M. hapla* is an obligate parasite, generation and maintenance of the F2 lines as living cultures is labor intensive and time consuming. Nonetheless, a consequence of the reproduction mechanism is that the F2 progeny resemble recombinant inbred lines. Due to this, sufficient DNA from each line is available for adding molecular markers to the genetic map or for further investigation of recombination intervals. Additionally, these lines can be maintained and utilized for phenotypic analysis. The availability of these lines provides a rare opportunity among parasitic nematodes to identify segregating traits of interest. The mapping of a trait for clumping behavior provides one example. Scorable differences in traits for attraction to and parasitism of particular hosts are segregating in these populations and quantitative trait loci responsible for these phenotypes have been identified (V. P. Thomas and V. M. Williamson, unpublished data). In the future, it should be possible to isolate the genes responsible for these and many other traits by utilizing the genetics tools we have developed and made available to the greater scientific community.

ACKNOWLEDGMENTS

The authors are grateful to Doug Cook, Richard Michelmore, and Varma Penmetsa for helpful discussions and to Herschel Espiritu, Mohit Bansal, David Xu, and Kiho Song for help with experiments. This work was supported by National Science Foundation Awards IOS-0744857 and IOS-1025840.

LITERATURE CITED

Atibalentja, N., S. Bekal, L. L. Domier, T. L. Niblack, G. R. Noel *et al.*, 2005 A genetic linkage map of the soybean cyst nematode *Heterodera glycines*. Mol. Genet. Genomics 273: 273–281.

Baker, B. S., A. T. Carpenter, M. S. Esposito, R. E. Esposito, and L. Sandler, 1976 The genetic control of meiosis. Annu. Rev. Genet. 10: 53–134.

Barnes, T. M., Y. Kohara, A. Coulson, and S. Hekimi, 1995 Meiotic recombination, noncoding DNA and genomic organization in *Caenorhabditis elegans*. Genetics 141: 159–179.

Bellafiore, S., Z. Shen, M. N. Rosso, P. Abad, P. Shih *et al.*, 2008 Direct identification of the *Meloidogyne incognita* secretome reveals proteins with host cell reprogramming potential. PLoS Pathog. 4: e1000192.

Beye, M., I. Gattermeier, M. Hasselmann, T. Gempe, M. Schioett *et al.*, 2006 Exceptionally high levels of recombination across the honey bee genome. Genome Res. 16: 1339–1344.

Bird, D. McK., 2005 Model systems in agriculture: lessons from a worm. Ann. Appl. Biol. 146: 147–154.

Chen, P., and P. A. Roberts, 2003 Genetic analysis of (a)virulence in *Meloidogyne hapla* to resistance in bean (*Phaseolus vulgaris*). Nematology 5: 687–697.

Chitwood, D. J., 2003 Research on plant-parasitic nematode biology conducted by the United States Department of Agriculture–Agricultural Research Service. Pest Manag. Sci. 59: 748–753.

Danchin, E. G. J., M. N. Rosso, P. Vieira, J. de Almeida-Engler, P. M. Coutinho *et al.*, 2010 Multiple lateral gene transfers and duplications have promoted plant parasitism ability in nematodes. Proc. Natl. Acad. Sci. USA 107: 17651–17656.

Davis, E. L., R. S. Hussey, M. G. Mitchum, and T. J. Baum, 2008 Parasitism proteins in nematode-plant interactions. Curr. Opin. Plant Biol. 11: 360–366.

Dong, K., and C. H. Opperman, 1997 Genetic analysis of parasitism in the soybean cyst nematode *Heterodera glycines*. Genetics 141: 1311–1318.

Fan, J. B., A. Oliphant, R. Shen, and B. G. Kermani, F. Garcia *et al.*, 2003 Highly parallel SNP genotyping. Cold Spring Harb. Symp. Quant. Biol. 68: 69–78.

Foley, J. A., N. Ramankutty, K. A. Brauman, E. S. Cassidy, J. S. Gerber *et al.*, 2011 Solutions for a cultivated planet. Nature 478: 337–342.

Goldstein, P., and A. C. Triantaphyllou, 1978 Karyotype analysis of *Meloidogyne hapla* by 3-D reconstruction of synaptonemal complexes from electron microscopy of serial sections. Chromosoma 70: 131–139.

Griffin, G. D., and M. V. McKenry, 1989 Susceptibility of Nevada synthetic XX germplasm to a California race of *Meloidogyne hapla*. J. Nematol. 21: 292–293.

Hill, W. G., and A. Robertson, 1966 The effect of linkage on limits to artificial selection. Genet. Res. 8: 269–294.

Hillers, K. J., and A. M. Villeneuve, 2003 Chromosome-wide control of meiotic crossing over in *C. elegans*. Curr. Biol. 13: 1641–1647.

Janssen, G., A. van Norel, and B. Verkerk-Bakker, and R. Janssen, 1997 Intra- and interspecific variation of root-knot nematodes, *Meloidogyne* spp. with regard to resistance in wild tuber-bearing *Solanum* species. Fundam. Appl. Nematol. 20: 449–457.

Katzer, F., R. Lizundia, D. Ngugi, D. Blake, and D. McKeever, 2011 Construction of a genetic map for *Theileria parva*: identification of hotspots of recombination. Int. J. Parasitol. 41: 669–675.

Lambert, K. N., K. D. Allen, and I. M. Sussex, 1999 Cloning and characterization of an esophageal-gland-specific chorismate mutase from the phytoparasitic nematode *Meloidogyne javanica*. Mol. Plant Microbe Interact. 12: 328–336.

Liu, Q. L., and V. M. Williamson, 2006 Host-specific pathogenicity and genome differences between inbred strains of *Meloidogyne hapla*. J. Nematol. 38: 158–164.

Liu, Q. L., V. P. Thomas, and V. M. Williamson, 2007 Meiotic parthenogenesis in a root-knot nematode results in rapid genomic homozygosity. Genetics 176: 1483–1490.

MacLeod, A., A. Tweedie, S. McLellan, and S. Taylor, N. Hall *et al.*, 2005 The genetic map and comparative analysis with the physical map of *Trypanosoma brucei*. Nucleic Acids Res. 33: 6688–6693.

Mitkowski, N. A., J. G. Van der Beek, and G. S. Abawi, 2002 Characterization of root-knot nematode populations associated with vegetables in New York State. Plant Dis. 86: 840–847.

Opperman, C. H., D. M. Bird, V. M. Williamson, D. S. Rokhsar, M. Burke *et al.*, 2008 Sequence and genetic map of *Meloidogyne hapla*: a compact nematode genome for plant parasitism. Proc. Natl. Acad. Sci. USA 105: 14802–14807.

Popeijus, H., H. Overmars, J. Jones, V. Blok, A. Goverse *et al.*, 2000 Degradation of plant cell walls by a nematode. Nature 406: 36–37.

Roberts, P. A., 1995 Conceptual and practical aspects of variability in root-knot nematode related host plant resistance. Annu. Rev. Phytopathol. 33: 199–221.

Rockman, M. V., and L. Kruglyak, 2009 Recombinational landscape and population genomics of *Caenorhabditis elegans*. PLoS Genet. 5: e1000419.

Ross, J. A., D. C. Koboldt, J. E. Staisch, H. M. Chamberlin, B. P. Gupta *et al.*, 2011 *Caenorhabditis briggsae* recombinant inbred line genotypes reveal inter-strain incompatibility and the evolution of recombination. PLoS Genet. 7: e1002174.

Rouppe van der Voort, J. N. A. M., H. J. van Eck, P. M. van Zandvoort, H. Overmars, J. Helder *et al.*, 1999 Linkage analysis by genotyping of sibling populations: a genetic map for the potato cyst nematode constructed using a "pseudo-F2" mapping strategy. Mol. Gen. Genet. 261: 1021–1031.

Sasser, J. N., 1980 Root-knot nematodes: a global menace to crop production. Plant Dis. 64: 36–41.

Sasser, J. N., and D. W. Freckman, 1987 A world perspective on nematology: the role of the society, pp. 7–14 in *Vistas on Nematology*, edited by J. A. Veech and D. W. Dickson. Society of Nematologists, Hyattsville, MD.

Scholl, E. H., J. L. Thorne, J. P. McCarter and D. McK. Bird, 2003 Horizontally transferred genes in plant-parasitic nematodes: a high-throughput genomic approach. Genome Biol. 4: R39.1–R39.12.

Stam, P., 1993 Construction of integrated genetic-linkage maps by means of a new computer package: JoinMap. Plant J. 3: 739–744.

Solignac, M., F. Mougel, D. Vautrin, M. Monnerot, and J. M. Cornuet, 2007 A third-generation microsatellite-based linkage map of the honey bee, *Apis mellifera*, and its comparison with the sequence-based physical map. Genome Biol. 8: R66.

Sommer, R. J., and A. Streit, 2011 Comparative genetics and genomics of nematodes: genome structure, development and lifestyle. Annu. Rev. Genet. 45: 1–20.

Su, Z., M. T. Ferdig, Y. Huang, C. Q. Huynh, A. Liu *et al.*, 1999 A genetic map and recombination parameters of the human malaria parasite *Plasmodium falciparum*. Science 286: 1351–1353.

Taylor, D. R., and P. K. Ingvarsson, 2003 Common features of segregation distortion in plants and animals. Genetica 117: 27–35.

Triantaphyllou, A. C., 1966 Polyploidy and reproductive patterns in the root-knot nematode *Meloidogyne hapla*. J. Morphol. 118: 404–414.

Triantaphyllou, A. C., 1973 Environmental sex differentiation of nematodes in relation to pest management. Annu. Rev. Phytopathol. 11: 441–462.

Triantaphyllou, A. C., and H. Hirschmann, 1980 Cytogenetics and morphology in relation to evolution and speciation of plant-parasitic nematodes. Annu. Rev. Phytopathol. 18: 333–359.

Trudgill, D. L., and V. C. Blok, 2001 Apomictic, polyphagous root-knot nematodes: exceptionally successful and damaging biotrophic root pathogens. Annu. Rev. Phytopathol. 39: 53–77.

Van der Beek, J., J. Los, and L. Pijanacker, 1998 Cytology of parthenogenesis of five *Meloidogyne* species. Fundam. Appl. Nematol. 21: 393–399.

Van Ooijen, J. W., 2006 *JoinMap 4: Software for the calculation of genetic linkage maps in experimental populations*. Kyazma B.V., Wageningen, The Netherlands.

Viney, M. E., and J. B. Lok, 2007 *Strongyloides* spp., *WormBook*, ed. The *C. elegans* Research Community WormBook, doi/10.1895/wormbook.1.141.1, http://www.wormbook.org.

Voorrips, R. E., 2002 MapChart: software for the graphical presentation of linkage maps and QTLs. J. Hered. 93: 77–78.

Vos, P., R. Hogers, M. Bleeker, M. Reijans, T. van de Lee *et al.*, 1995 AFLP: a new technique for DNA fingerprinting. Nucleic Acids Res. 23: 4407–4414.

Wang, C., S. Lower, V. P. Thomas, and V. M. Williamson, 2010 Root-knot nematodes exhibit strain-specific clumping behavior that is inherited as a simple genetic trait. PLoS ONE 5: e15148.

Wilfert, L., J. Gadau, and P. Schmid-Hempel, 2007 Variations in genomic recombination rates among animal taxa and the case of social insects. Heredity 98: 189–197.

Williamson, V. M., and C. A. Gleason, 2003 Plant-nematode interactions. Curr. Opin. Plant Biol. 6: 327–333.

Communicating editor: D. G. Moerman